Heliyon 10 (2024) e31586

Contents lists available at ScienceDirect

Heliyon

journal homepage: www.cell.com/heliyon

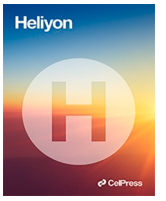

Research article

# High expression of CCNB2 is an independent predictive poor prognostic biomarker and correlates with immune infiltrates in breast carcinoma

Zonghong Lu [a], Zhihong Wang [b], Guodong Li [b,*]

[a] *Department of Thyroid and Breast Surgery, Tongji Hospital, Tongji Medical College, Huazhong University of Science and Technology, Wuhan, Hubei, 430030, China*

[b] *Tongji Hospital of Tongji Medical College of Huazhong University of Science and Technology, GI Cancer Research Institute, Wuhan, Hubei, 430030, China*

ARTICLE INFO

*Keywords:*
Cyclin B2 (CCNB2)
Breast carcinoma (BRCA)
Tumor microenvironment
Immune infiltrate
Immune checkpoint
Tumor mutational burden
Prognosis

ABSTRACT

*Background:* Cyclin B2 (CCNB2) is associated with cell cycle progression, acting as a cell cycle checkpoint in progression of G2/M transition. In many cancer patients, it has been observed that overexpression of CCNB2 enhances tumor invasiveness and leads to adverse prognosis. However, the association of CCNB2 with the tumor microenvironment remains unclear. Therefore, it is necessary to clarify the associations of CCNB2 with the immune status and prognosis of breast carcinoma (BRCA).

*Methods:* Gene expression and clinical data for BRCA were obtained from The Cancer Genome Atlas and Gene Expression Omnibus databases, followed by association analyses of CCNB2 expression with prognosis, immune cell infiltration, and immune checkpoints. This study further performed drug sensitivity analysis and constructed a prognostic nomogram for CCNB2.

*Results:* 3619 differentially expressed genes were identified in BRCA, including CCNB2 that emerged as a key gene in the network. High CCNB2 expression correlated with poor prognosis. Functional analysis demonstrated enrichment of CCNB2 co-expressed genes with the cell cycle, cancer progression, cell energy, and immune pathways. Microsatellite instability and tumor mutation burden analyses indicated CCNB2 as a candidate immunotherapy target. Tumor-infiltrating myeloid-derived suppressor cells, regulatory T cells, and T helper 2 cells were associated with CCNB2-related tumor progression and metastasis. CCNB2 expression positively correlated with immune checkpoints, indicating that high CCNB2 expression might facilitate tumor immune escape. Tumors with high CCNB2 expression showed sensitivity to phosphoinositide 3-kinase-protein kinase B-mammalian target of rapamycin and cyclin-dependent kinase (CDK) 4/6 inhibitors, and the nomogram had good prognostic predictive ability for patients with BRCA.

*Conclusions:* CCNB2 may play a crucial role in tumorigenesis and serve as an independent prognostic biomarker associated with tumor microenvironment, tumor immune infiltration and immunotherapy in BRCA.

* Corresponding author. Tongji Hospital of Tongji Medical College of Huazhong University of Science and Technology, GI Cancer Research Institute, 1095 Jiefang Avenue, Qiaokou District, Wuhan, Hubei 430030, China.
*E-mail address:* gdli1986@163.com (G. Li).

https://doi.org/10.1016/j.heliyon.2024.e31586
Received 12 March 2024; Received in revised form 17 May 2024; Accepted 20 May 2024
Available online 21 May 2024

**Abbreviations**

| | |
|---|---|
| DLBC | Lymphoid Neoplasm Diffuse Large B-cell Lymphoma |
| STAD | Stomach adenocarcinoma |
| ACC | Adrenocortical carcinoma |
| PAAD | Pancreatic adenocarcinoma |
| KICH | Kidney Chromophobe |
| LUAD | Lung adenocarcinoma |
| BRCA | Breast carcinoma |
| LGG | Brain Lower Grade Glioma |
| PRAD | Prostate adenocarcinoma |
| SARC | Sarcoma |
| BLCA | Bladder Urothelial Carcinoma |
| UCEC | Uterine Corpus Endometrial Carcinoma |
| COAD | Colon adenocarcinoma |
| LUSC | Lung squamous cell carcinoma |
| THYM | Thymoma |
| DEGs | Differentially expressed genes |
| GO | Gene ontology |
| KEGG | Kyoto encyclopedia of genes and genomes |
| GSEA | Gene set enrichment analysis |
| TCGA | The cancer genome atlas |
| GEO | Gene Expression Omnibus |
| OS | Overall survival |
| RFS | Recurrence free survival |
| HER2 | Human epidermal growth factor receptor 2 |
| TME | Tumor microenvironment |
| TIICs | Tumor-infiltrating immune cells |
| PPI | Protein–protein interaction |
| MSI | Microsatellite instability |
| TMB | Tumor mutation burden |

## 1. Introduction

Breast carcinoma (BRCA) is the most commonly diagnosed cancer and the fifth leading cause of cancer-related deaths in women [1], including in China [2], where over 2 million women were diagnosed with BRCA in 2020 and the disease caused 685,000 deaths [1,3]. Despite notable improvements in diagnosis and treatment, the prognosis of some patients with BRCA remains poor [4]. Immunohistochemical BRCA classification primarily relies on human epidermal growth factor receptor 2 (HER2), progesterone receptor, and estrogen receptor expression [5,6]. Therefore, BRCA is classified into subtypes such as normal-like, HER2-enriched, luminal A, luminal B, and basal-like [7–9]. Triple-negative breast cancer (TNBC), known for its poorest prognosis, constitutes approximately 15 % of breast cancer subtypes [10]. At present, the standard treatment regimen for BRCA comprises radiation, hormone and targeted therapies, chemotherapy, and surgery, and various drug combinations and targeted treatments have shown promising outcomes [11]. Despite the considerable progress in BRCA treatment, endocrine therapy resistance remains a significant challenge [12]. Chemotherapy continues to be the standard treatment for advanced triple-negative breast cancer owing to the absence of specific therapeutic targets [13]. However, conventional chemotherapy drugs have limited efficacy in improving the pathological complete response rates [14], patients with distant metastases still exhibit a median overall survival of less than two years [15,16]. Therefore, continued investigations into the underlying mechanisms of carcinogenesis and new therapeutic approaches for BRCA are crucial.

The tumor microenvironment (TME) is one of the important parts of cancer occurrence and development, which can weaken immune surveillance and induce tumor resistance [17]. Immunotherapy, which plays a role by enhancing anti-tumor immune response, is one of the important directions in the research of breast cancer treatment [18]. Targeted therapies, especially for immune checkpoints, are promising BRCA treatment options [19]. Previous studies have demonstrated that immune activation improves the prognosis of HER2-positive and triple-negative BRCAs [20]. Furthermore, preliminary findings from a study using programmed cell death (PD)-1/PD-ligand 1 antagonists demonstrated that certain BRCA subtypes possess inherent immunogenicity, resulting in sustained overall responses in some patients. Nevertheless, the clinical efficacy of monotherapy is limited, providing benefits to only a minority of patients who developed metastatic diseases [21]. Therefore, identifying novel and reliable immune-related biomarkers for BRCA is imperative.

CCNB2 is a pivotal member of the cyclin family with a crucial role in regulating cell cycle progression, acting as a cell cycle checkpoint. The aberrant expression of cyclin family members frequently contributes to tumorigenesis. For example, high cyclin B1 (CCNB1) expression affects prostate cancer development and elicits tumor resistance [22]. Similarly, cyclin E1 (CCNE1) is a potential

target for ovarian carcinoma treatment [23]. High CCNB2 expression occurs in breast cancer tissues and is correlated with a poor prognosis [24–26]. In recent years, some studies have found a close association between members of the cyclin family and the tumor microenvironment. CCNG2, previously demonstrated to have tumor cell proliferation inhibitory effects, has recently been found to reverse immune suppression in the tumor microenvironment of glioma cells and enhance the blockade effect of PD-1 [27,28]; furthermore, overexpression of the cyclin D1b can mediate breast cancer cells to regulate macrophage differentiation into a more immunosuppressive M2 phenotype, demonstrating its importance in the tumor microenvironment [29,30]. However, the precise relationship between CCNB2 and the specific mechanisms underlying cancer initiation and progression, particularly regarding the TME and tumor-infiltrating immune cells (TIICs), remains elusive.

Therefore, this study analyzed differentially expressed genes (DEGs) between BRCA and normal tissues to assess correlations between key genes (including CCNB2) and prognosis, immune checkpoints, and potential mechanisms to provide insights and targets for novel BRCA therapies.

## 2. Materials and methods

### 2.1. Data sources and processing

The RNA-sequencing data and corresponding clinical information of 33 cancer cases were retrieved from The Cancer Genome Atlas (TCGA, https://portal.gdc.cancer.gov/) portal. All data were downloaded and standardized using the "TCGAbiolinks" R package (version 2.29.0) [31]. Patients with an unsatisfactory sample state, incomplete clinical information, or incomplete survival data were excluded. In total, 1080 BRCA and 99 adjacent normal tissue samples were included in the mRNA expression analyses and 963 BRCA samples were included in the survival analyses.

In addition, two independent expression microarray datasets containing gene expression data and BRCA clinical profiles were retrieved from the Gene Expression Omnibus (GEO, https://www.ncbi.nlm.nih.gov/geo/) database (GSE42568 and GSE65194). R software (Version 4.3.1, https://cran.r-project.org/bin/windows/base/old/4.3.1/) and the "ggplot2" R-package (Version 3.4.2, https://ggplot2.tidyverse.org) were used for the statistical analyses and data visualization, respectively.

### 2.2. Somatic mutation analysis

Somatic cell mutation data were obtained from TCGA database. "Masked Somatic Mutation" data were selected and processed using the R package "TCGAbiolinks." The single nucleotide polymorphism mutation annotation format was analyzed with the "maftools" R package (version 2.16.0), which provides various approaches for visualization [32].

### 2.3. DEG identification and survival analyses

The "DESeq2" (version 1.38.3) and "limma" (version 3.54.2) R packages were used to screen DEGs between normal breast tissue and tumor tissue samples in TCGA-BRCA cohort and GSE42568 dataset [33,34]; genes with a $|\log2 \text{ (fold change)}| > 1$ in expression level between groups were identified as significant DEGs. Subsequently, The survival analysis was conducted utilizing the "survival" R package (version 3.5.5, https://CRAN.R-project.org/package=survival) to determine genes significantly associated with overall survival; candidate genes were identified using the "VennDiagram" R package (version 1.7.3) [35]. Functional enrichment analysis for Gene Ontology (GO) terms and Kyoto Encyclopedia of Genes and Genomes (KEGG) pathways was further conducted using the "clusterProfiler" R package (version 4.8.1) [36]. Statistical significance was set at $P < 0.05$.

### 2.4. Protein–protein interaction (PPI) network construction

The candidate DEGs were incorporated in construction of a PPI network using the STRING website (https://cn.string-db.org/). The criteria for further screening were "physical subnetwork", "highest confidence (0.900)" and "hide disconnected nodes in the network". After deleting all free nodes, 17 hub genes were identified for further evaluation.

### 2.5. CCNB2 expression and prognostic significance

TCGA-BRCA cohort data were used to assess CCNB2 expression levels in BRCA tissues. The TIMER 2.0 tool was also used to visualize CCNB2 expression levels in pan-cancer [37]. Patients were categorized into $CCNB2^{high}$ and $CCNB2^{low}$ groups based on the median expression level. Kaplan–Meier plots of the association of CCNB2 expression with overall survival were visualized utilizing the "survival" and "survminer" R packages (version 0.4.9, https://CRAN.R-project.org/package=survminer).

Gene expression and survival data from the GSE42568 dataset were also retrieved from the GEO database to verify the results obtained with TCGA data. The Kaplan–Meier Plotter (http://kmplot.com/analysis/) website and the Human Protein Atlas database (HPA, https://www.proteinatlas.org/) were used for the prognostic analysis and protein expression validation, respectively.

### 2.6. CCNB2 co-expression and functional enrichment analyses

Pearson's method was employed to identify genes co-expressed with CCNB2 (correlation coefficient of $>0.6$ or $< -0.4$) in BRCA

tissues, and GO and KEGG enrichment analyses were used to elucidate the functional implications of the co-expressed genes. Gene set enrichment analysis (GSEA) was used to analyze the potential molecular mechanisms enriched in the co-expressed genes (|normalized enrichment score| >1). A false discovery rate of <0.05 and a p-value of <0.05 were considered statistically significant. The "h.all.v2023.1. Hs.entrez.gmt" gene set was used as a reference.

The GO and KEGG analysis results were visualized as a circle plot using the "ComplexHeatmap" (version 2.16.0) and "circlize" (0.4.15) R packages [38,39], while the GSEA results were visualized using the "enrichplot" R package (version 1.20.0, https://doi.org/10.18129/B9.bioc.enrichplot). The PPI network between CCNB2 and the co-expressed genes (correlation coefficient >0.8 or < –0.4, p < 0.05) was analyzed using the STRING website and constructed in Cytoscape [40,41].

### 2.7. Relationships between CCNB2 expression and TIICs

This research investigated the associations between CCNB2 expression and the signature genes of 28 types of immune cells using single-sample GSEA (ssGSEA) with the "IOBR" R package (version 0.99.9) [42]. TCGA results were validated using the GSE65194 GEO dataset and Molecular Taxonomy of Breast Cancer International Consortium (METABRIC, https://www.bccrc.ca/dept/mo/) data. The TIICs in the $CCNB2^{high}$ and $CCNB2^{low}$ groups were compared using the Wilcoxon test and Spearman's correlation analysis.

### 2.8. Microsatellite instability (MSI), tumor mutation burden (TMB), immune checkpoint, and chemokine analyses

The relationships between CCNB2 expression and MSI or TMB were also investigated. The "cBioPortalData" R package (version 2.12.0) was used to obtain MSI scores in pan-cancer data from TCGA [43]. The masked somatic mutation data from TCGA were used to determine the TMB score for each cancer type. In addition, this study explored the associations between CCNB2 and the currently recognized major immune checkpoints. The analyses evaluated the correlations between CCNB2 expression and MSI, TMB, and the immune checkpoint molecules using Spearman's correlation coefficient. Finally, this study assessed the correlations between CCNB2 expression and the levels of chemokines, including receptor and ligand families, utilizing the Tumor Immune System Interaction Database (TISIDB) [44].

### 2.9. Drug sensitivity analysis

The "Oncopredict" R package (version 0.2) was employed to predict drug sensitivity in patients with BRCA using tumor therapy genome data [45]. The half-maximal inhibitory concentration (IC50) and area under the concentration–response curve (AUC) values were obtained from the Genomics of Drug Sensitivity in Cancer database [46].

### 2.10. Cell culture

Human breast cancer cell line (MDA-MB-231 and MCF-7) were obtained from American Type Culture Collection (ATCC; Manassas; VA). MDA-MB-231 was cultured in DMEM medium (HyClone, Logan, UT, USA) supplemented with 10 % fetal bovine serum (FBS) at 37 °C and 5 % CO2. MCF-7 was cultured in MEM medium (HyClone, Logan, UT, USA) supplemented with 10 % FBS and 10ug/ml insulin at 37 °C and 5 % CO2.

### 2.11. Reverse transcription-quantitative polymerase chain reaction (RT-qPCR)

Clinical samples were obtained from the Wuhan Tongji Hospital. RT-qPCR was conducted using SYBR® Green (Roche, Basel, Switzerland) for quantification of gene expression. The $2^{-\Delta\Delta Ct}$ method was used to determine the relative expression levels of CCNB2; GAPDH served as the control gene. Statistical analyses were performed using GraphPad Prism (Version 9.1.0; GraphPad Software, San Diego, CA, USA), and a p-value <0.05 was considered statistically significant. Table 1 lists the primer sequences used in RT-qPCR.

### 2.12. Western blotting

Following cell lysis using RIPA lysis buffer, total protein was isolated, resolved on a sodium dodecyl sulfate-polyacrylamide gel, subsequently transferred onto polyvinylidene fluoride membranes and incubated with primary antibodies for GAPDH (AC033; ABclonal) and CCNB2 (ab185622; Abcam).

**Table 1**
RT-qPCR primer sequences of GAPDH and CCNB2.

| | Forward Primer | Reverse Primer |
|---|---|---|
| CCNB2 | CCGACGGTGTCCAGTGATTT | TGTTGTTTTGGTGGGTTGAACT |
| GAPDH | GGAGCGAGATCCCTCCAAAAT | GGCTGTTGTCATACTTCTCATGG |

### 2.13. Colony formation assay

Normal breast cancer cells and cells stably transfected with sg-CCNB2 were seeded in a 6-well culture plate. The culture medium was renewed every 48 h, and the cells were maintained in culture for a duration of 7 days. Subsequently, the cellular clones were fixed using 4 % paraformaldehyde, stained with 0.1 % crystal violet, and enumerated manually.

### 2.14. Transwell assay

The invasiveness of breast cancer cells was assessed utilizing Transwell insert chambers (Corning, NY, USA) that had been pre-coated with Matrigel (Corning Inc.). Specifically, $2*10^4$ cells were inoculated into the upper chamber containing 200 μl of serum-free medium, while 500 μl of culture medium supplemented with 20 % FBS was introduced into the lower chamber. Following a 24-h incubation period, the invaded cells were fixed using 4 % paraformaldehyde and subsequently stained with 0.1 % crystal violet.

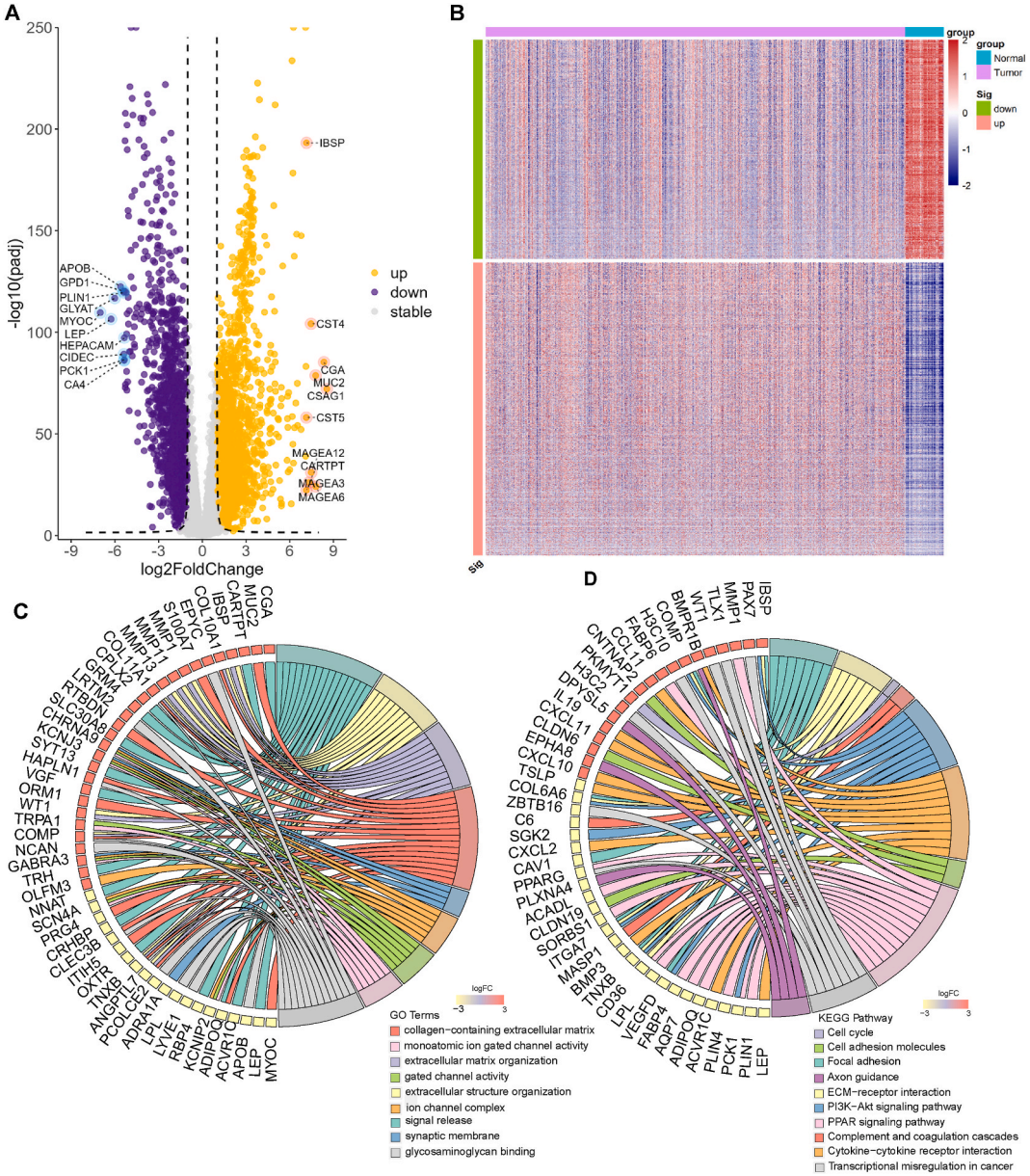


**Fig. 1. DEG analysis and functional enrichment in BRCA. (A)** Volcano plot of 2069 significantly upregulated and 1550 significantly downregulated DEGs. **(B)** Heat map of DEGs between BRCA and adjacent normal breast tissues. **(C–D)** Chordal plots of the functional enrichment analyses of DEGs, including GO enrichment analysis **(C)** and KEGG analysis **(D)**.

Enumeration of cells was conducted under a microscope, and the count was performed for five randomly selected fields at a magnification of 100 × .

### 2.15. Nomogram construction and evaluation

Univariate and multivariate Cox regression analyses were used to identify significant independent prognostic factors for BRCA. The "survival" R package was utilized for survival data analyses, and the results were visualized using the "forestplot" R package (version 3.1.1, https://CRAN.R-project.org/package=forestplot). Significant prognostic factors were used to construct a nomogram to evaluate the 1-, 3-, 5-, and 7-year overall survival probabilities of patients with BRCA. The "rms" R package (version 6.7.0, https://CRAN.R-project.org/package=rms) was used to create the nomogram. The receiver operating characteristic (ROC) curve was used to assess the predictive performance of the model. A calibration curve was created to illustrate the model's accuracy according to the reference line.

### 2.16. Statistical analyses

Student's t-test was utilized to detect differences between groups. Spearman's and Pearson's coefficients were used to evaluate


**Fig. 2. BRCA mutation landscape.** **(A)** Gene counts of different variant classification. **(B)** Gene counts of different variant type. **(C)** Gene counts of different SNV classification. **(D)** Total mutation number in each sample. **(E)** Variant classification in each sample. **(F)** Top 10 mutated genes. **(G–H)** Waterfall plots of top mutated genes in TCGA gene set **(G)** and DEGs **(H)**. Samples were classified according to pam50 subtype, pathologic stage, pathologic subtype and vital status.

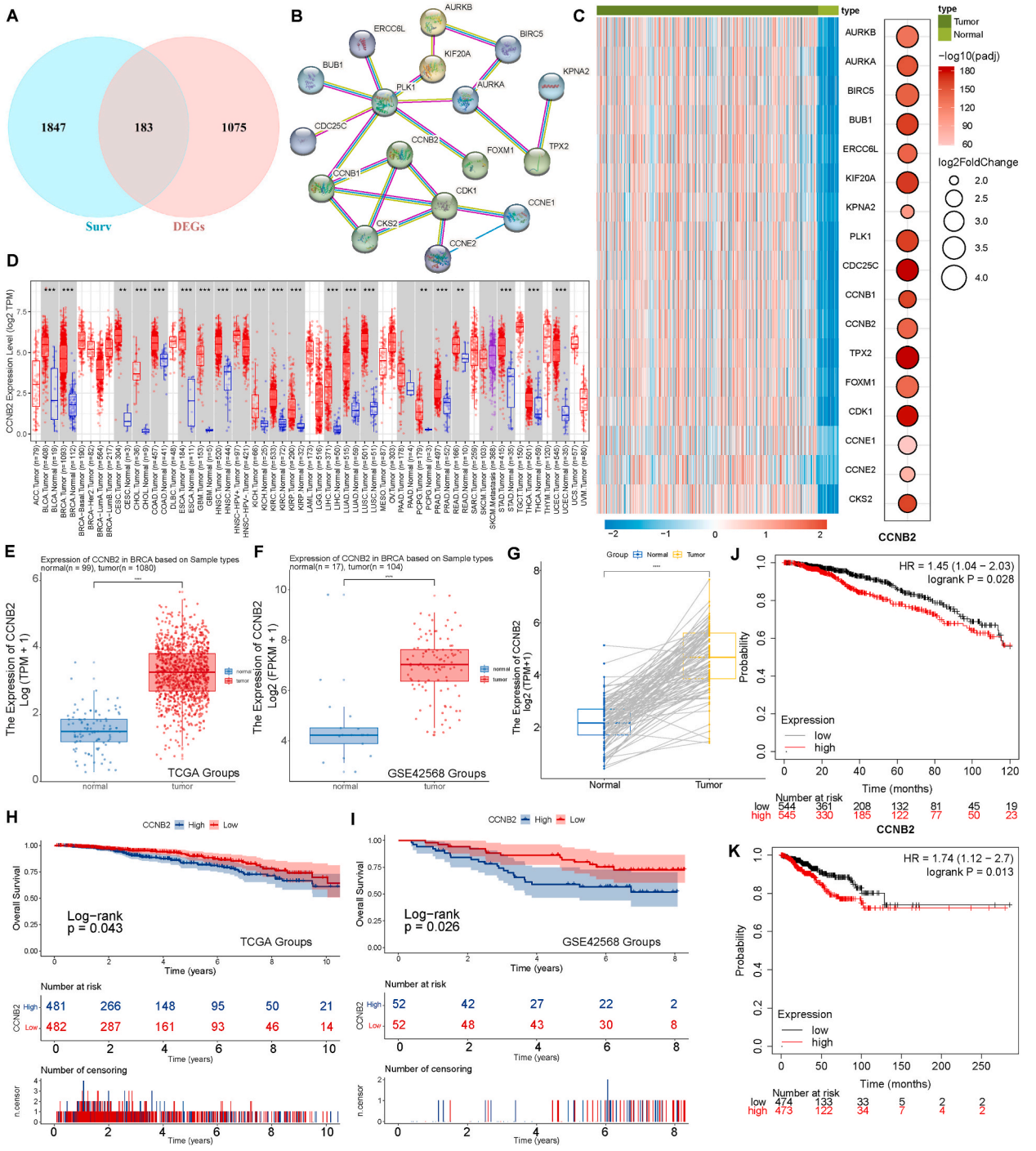


**Fig. 3. Identify CCNB2 as a hub DEG related to the prognosis of patients with BRCA. (A)** Venn plot of 183 prognosis-related DEGs. **(B)** PPI network of hub genes. **(C)** Combination of heat map and bubble plot showing expression, FoldChange value and adjust p-value of hub genes. **(D)** Expression of CCNB2 in pan-cancer from TIMER 2.0 database. **(E)** Expression of CCNB2 between normal (n = 99) and tumor (n = 1080) tissues in TCGA-BRCA. **(F)** Expression of CCNB2 between normal (n = 17) and tumor (n = 104) tissues in GSE42568. **(G)** CCNB2 mRNA level in tumor tissues and matched normal breast tissues in TCGA-BRCA. **(H–I)** Kaplan-Meier survival curves of overall survival rate of $CCNB2^{high}$ and $CCNB2^{low}$ in TCGA-BRCA **(H)** and GSE42568 **(I)**. **(J–K)** Kaplan-Meier survival curves from Kaplan-Meier plotter Kaplan–Meier Plotter showing overall survival rate **(I)** and disease-free survival rate **(J)** of $CCNB2^{high}$ and $CCNB2^{low}$ of patients with BRCA.

correlations as appropriate. All statistical analyses were performed using R software, and a p-value of $<0.05$ was considered statistically significant.

## 3. Results

### 3.1. DEG identification and functional annotation

The DEG analysis identified 2069 significantly upregulated and 1550 significantly downregulated genes in TCGA-BRCA cohort (Fig. 1A and B). The GO enrichment analysis (Fig. 1C) determined that the DEGs were involved in signal release, collagen-containing extracellular matrix, and gated channel activity processes. The KEGG analysis (Fig. 1D) demonstrated significant enrichment of cell cycle, extracellular matrix-receptor interaction, and focal adhesion pathways.

### 3.2. BRCA mutation landscape

Missense mutations were the primary type of mutations observed in patients with BRCA (Fig. 2A). Single nucleotide polymorphisms were more frequent than insertions or deletions (Fig. 2B). Notably, C > T substitutions were the most prevalent form of single-nucleotide variants in BRCA (Fig. 2C). Fig. 2D and E illustrate the other mutation types and information within BRCA, and Fig. 2F and G illustrate the mutation information of the gene set and DEGs.

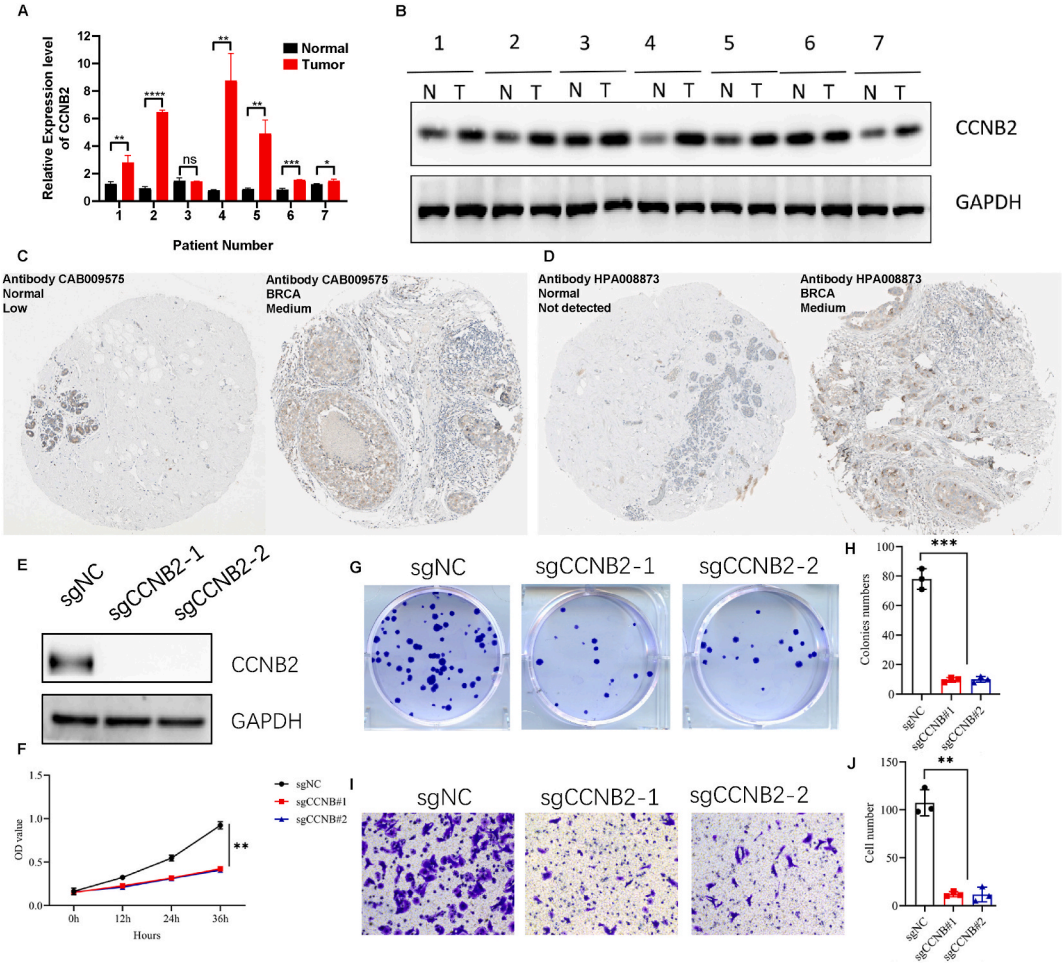


**Fig. 4. Experimental validation of CCNB2 expression level. (A)** RT-qPCR detecting the mRNA expression level of CCNB2 in BRCA tissues and adjacent normal tissues. **(B)** Western blot detecting the protein expression level of CCNB2 in BRCA tissues and adjacent normal tissues. Western blot results were cropped from adjacent lanes on the same gel in the same experiment. **(C–D)** Immunohistochemistry detecting the protein expression level of CCNB2 in BRCA tissues and normal tissues from the HPA database. **(E–F)** Protein expression level and gene expression level of CCNB2 in control and knockdown group. Western blot results were cropped from adjacent lanes on the same gel in the same experiment. **(G–H)** Colony formation assay were performed, and number of colony formation assessed of the indicated breast cancer cells which control or Knockdown CCNB2. **(I–J)** Transwell assays were performed to evaluate the effects of CCNB2 on the migration of the indicated breast cancer cells.

The top five genes with the highest mutation rates in BRCA were *TP53* (34 %), *PIK3CA* (34 %), *TTN* (17 %), *CDH1* (13 %), and *GATA3* (13 %). Similarly, the top five DEGs with the highest mutation rates in BRCA were *TTN* (17 %), *GATA3* (13 %), *SYNE1* (6 %), *ZFHX4* (5 %), and *DMD* (5 %).

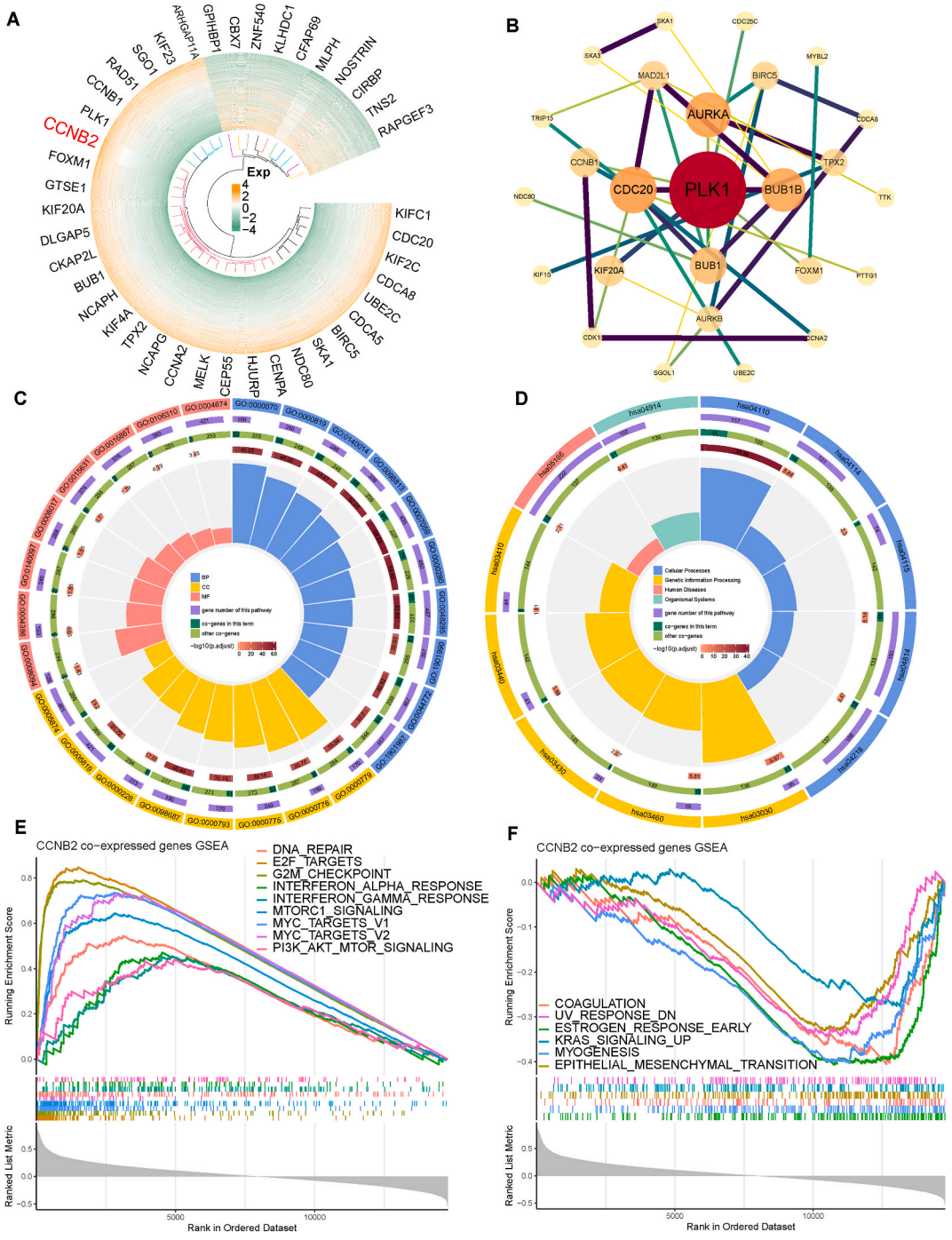


**Fig. 5. Genes co-expressed with CCNB2 and functional annotation. (A)** Circle heat map of the expression level of genes co-expressed with CCNB2. **(B)** Protein-protein interaction network of the co-expressed genes. **(C–D)** Multidimensional circle plots of the functional annotation of the co-expressed genes using GO enrichment analysis **(C)** and KEGG analysis **(D)**. **(E–F)** The GSEA results of pathways positively **(E)** and negatively **(F)** enriched of CCNB2 co-expressed genes.

### 3.3. Survival and PPI network analyses

This study also verified the prognostic value of the DEGs by survival analysis with TCGA data. In total, 1847 genes related to prognosis were identified, 183 of which intersected with the identified DEGs (85 downregulated and 98 upregulated) (Fig. 3A). Moreover, the STRING database was used to ascertain the interactions among the intersecting genes by constructing PPI networks to identify hub genes (Fig. 3B) and differential expression of the hub genes (Fig. 3C). *CCNB2* was a differentially expressed hub gene; therefore, further analyses were performed with *CCNB2* since its role in immune infiltration and the TME remains unclear.

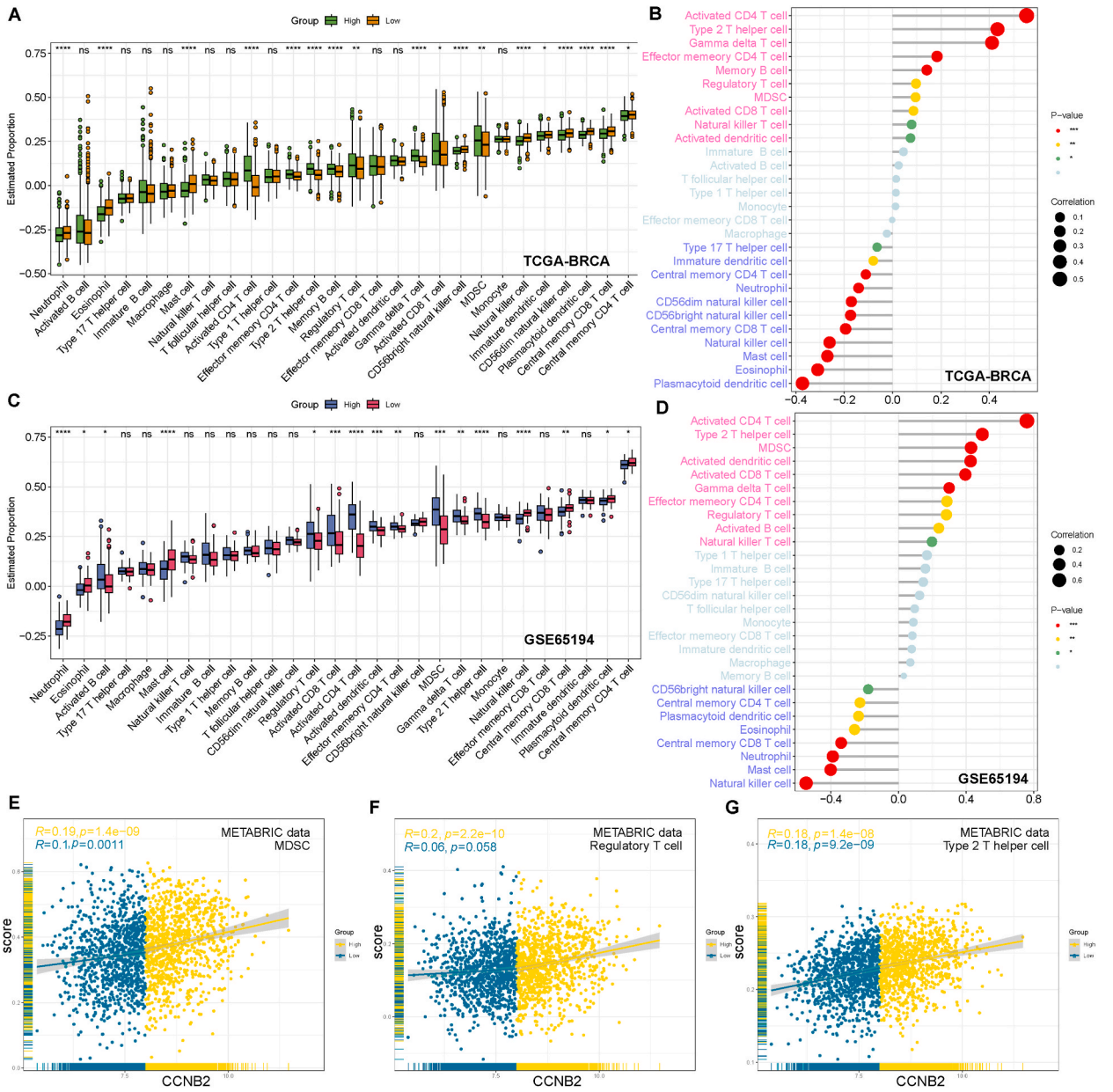


**Fig. 6. Correlation analysis between CCNB2 expression and immune infiltration in BRCA. (A)** Boxplot of estimated proportion of TIICs in CCNB2$^{high}$ and CCNB2$^{low}$ in TCGA-BRCA. **(B)** Lollipop plot of the correlation between CCNB2 expression level and TIICs in TCGA-BRCA. **(C)** Boxplot of estimated proportion of TIICs in CCNB2$^{high}$ and CCNB2$^{low}$ in GSE65194. (D) Lollipop plot of the correlation between CCNB2 expression level and TIICs in GSE65194. (E–**G)** Scatter plots of the correlation between CCNB2 expression level and MDSC, Treg and Th2 in CCNB2$^{high}$ and CCNB2$^{low}$ in METABRIC database. *P < 0.05, **P < 0.01, ***P < 0.001, ns, no significance.

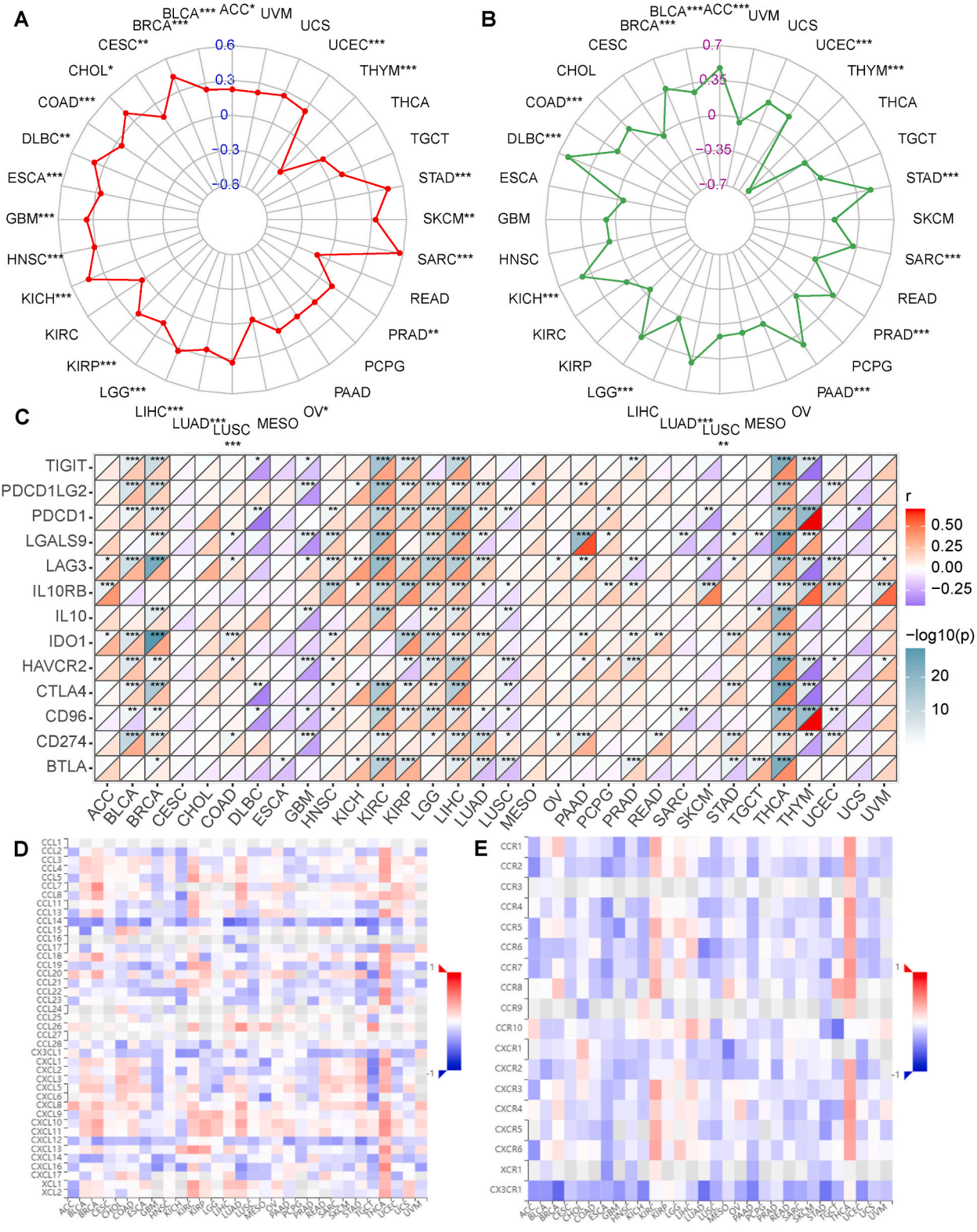


**Fig. 7. MSI, TMB, immune checkpoint, and chemokines pan-cancer analysis. (A–B)** Radar plots of the correlation between CCNB2 expression level and MSI **(A)** or TMB **(B)** in pan-cancer. **(C)** Diagonal heat map of the correlation between CCNB2 expression level and immune checkpoints in pan-cancer. **(D–E)** Heat maps of the correlation between CCNB2 expression level and chemokine legend **(D)** and receptor **(E)** families from TISIDB database. *P < 0.05, **P < 0.01, ***P < 0.001, ns, no significance.

### 3.4. Association of CCNB2 expression with BRCA prognosis

*CCNB2* expression was significantly upregulated in most tumors compared to the normal controls in pan-cancer analysis of TCGA database, especially in BRCA (Fig. 3D–E). Further analysis of the 98 paired BRCA and normal adjacent samples from TCGA database verified that *CCNB2* mRNA expression was higher in the BRCA samples than in the normal samples (Fig. 3G).

This research further assessed the effects of *CCNB2* expression on the survival outcomes of patients with BRCA using TCGA data. The *CCNB2*$^{high}$ group had significantly shorter overall survival than the *CCNB2*$^{low}$ group (Fig. 3H, $p = 0.043$), suggesting that *CCNB2* functions as an oncogene in BRCA and its overexpression indicates a worse prognosis.

The study separately validated the results obtained from TCGA data using the GSE42568 dataset, demonstrating elevated *CCNB2* expression in BRCA tissues and an association with poor prognosis (Fig. 3F and I, $p = 0.026$). The prognostic result was further confirmed by a survival analysis assessing overall survival and relapse-free survival (Fig. 3J–K, $p = 0.028$ and $p = 0.013$, respectively). Moreover, *CCNB2* expression based on RT-qPCR (Fig. 4A), western blotting (Fig. 4B and Supplementary Figs. 4A–B), and HPA database (Fig. 4C and D) analyses confirmed the difference between normal and tumor tissues. Subsequently, analyses investigated the impact of *CCNB2* gene expression on tumor proliferation (Fig. 4E–F and Supplementary Figs. 4C–D). The *CCNB2* knockdown group exhibited a significant inhibition of tumor proliferation (Fig. 4G–H) and migration (Fig. 4I–J) compared to the control group. Similar to the findings in the triple-negative breast cancer cell line MDA-MB-231, knockdown of *CCNB2* inhibited the proliferation and migration of hormone receptor-positive breast cancer cell line MCF-7 (Supplementary Fig. 1 and 4E-F).

### 3.5. Genes co-expressed with CCNB2 in BRCA

Next, genes were identified co-expressed with *CCNB2* using RNA-sequencing data from patients with BRCA in TCGA database. Fig. 5A presents a circular heat map of the top 30 positively correlated genes and the top 10 negatively correlated genes with *CCNB2*. Fig. 5C and D presents the GO and KEGG enrichment analysis results, respectively (Supplementary Tables 1–2).

Chromosome segregation, chromosomal region, and tubulin binding were the most significantly enriched GO terms for biological processes, cellular components, and molecular function, respectively. Similarly, cell cycle, DNA replication, cellular senescence, the p53 signaling pathway, and mismatch repair were the main enriched KEGG pathways associated with BRCA. The PPI network analysis demonstrated that the genes most related to *CCNB2* at the protein level were *PLK1*, *CDC20*, *AURKA*, *BUB1B*, and *BUB1* (Fig. 5B and Supplementary Fig. 2).

The pathways of *CCNB2* co-expressed genes were analyzed by GSEA (Fig. 5E and F and Supplementary Table 4), suggesting that the co-expressed genes were positively associated with cell cycle-related pathways (E2F-targets, G2/M phase checkpoint, master regulator of cell cycle entry and proliferative metabolism [MYC] targets v1/v2, and mitotic spindle), cancer-related pathways (mammalian target of rapamycin complex 1 [mTORC1] and phosphoinositide 3-kinase-protein kinase B-mammalian target of rapamycin [PI3K-Akt-mTOR] signaling), cell energy-related pathways (reactive oxygen species [ROS], oxidative phosphorylation, and glycolysis), DNA repair, and the interferon response in the hallmark gene set (Supplementary Table 3). In addition, the co-expressed genes exhibited negative associations with myogenesis, early estrogen response, coagulation, down-regulated ultraviolet response, and upregulated Kirsten rat sarcoma virus (KRAS) signaling. Interestingly, these genes were also negatively enriched in the epithelial–mesenchymal transition pathway.

### 3.6. Tumor immune infiltration analyses

The infiltration of immune cells into tumor tissues is an independent prognostic factor for survival in most malignant tumors. Consequently, analyses examined the correlations between *CCNB2* and TIICs in BRCA using ssGSEA (Fig. 6A and Supplementary Table 5). *CCNB2* expression was positively associated with myeloid-derived suppressor cell (MDSC) infiltration, activated cluster of differentiation (CD)8+ T cells, gamma delta T cells, regulatory T cells (Tregs), memory B cells, type 2 T helper cells (Th2), effector memory $CD4^+$ T cells, and activated $CD4^+$ T cells. Furthermore, *CCNB2* expression was negatively associated with the infiltration of central memory $CD8^+$ T cells, central memory $CD4^+$ T cells, plasmacytoid dendritic cells (pDCs), CD56dim natural killer (NK) cells, CD56bright NK cells, NK cells, immature dendritic cells, mast cells, eosinophils, and neutrophils.

Fig. 6B also depicts the associations between *CCNB2* expression and TIICs. Most importantly, the study identified a positive association between *CCNB2* and TIICs that are known to promote tumor development and aggression in the TME, such as MDSCs, Tregs, and Th2 cells. In addition, NK cells, including CD56dim and CD56bright cells, were suppressed the most by high *CCNB2* expression.

These associations were verified in the GSE65194 dataset (Fig. 6C and D) and the METABRIC database (Fig. 6E–G), confirming that high *CCNB2* expression is inextricably linked with TME changes and decreased NK cells.

### 3.7. MSI, TMB, immune checkpoint, and chemokines pan-cancer analysis

MSI is a hypermutation phenotype resulting from the loss of DNA mismatch repair activity, which serves as a molecular marker for a deficient mismatch repair system. Positive interactions between *CCNB2* and MSI were observed in most human cancers, whereas a negative interaction was observed exclusively in THYM (Fig. 7A). The TMB has emerged as a reliable marker for predicting the sensitivity to block immune checkpoints. This study revealed a remarkable positive correlation between *CCNB2* and the TMB in several cancer types, including DLBC, STAD, ACC, PAAD, KICH, LUAD, BRCA, LGG, PRAD, SARC, BLCA, UCEC, COAD, and LUSC. In contrast, *CCNB2* expression was negatively correlated with TMB only in THYM (Fig. 7B).

Next, this research analyzed the association between *CCNB2* and immune checkpoint molecules (Fig. 7C). Further analysis in BRCA illustrated that *CCNB2* expression correlated significantly with immune checkpoints (Supplementary Fig. 3). Additionally, analyses identified a significant association between *CCNB2* and various chemokine family molecules in BRCA (Fig. 7D and E). *CCNB2* expression was most negatively associated with C-X3-C motif chemokine receptor 1 (CX3CR1), C–C motif chemokine ligand (CCL) 14, C-X-C motif chemokine ligand (CXCL) 12, CXCL14, and C–C motif chemokine receptor 6 (CCR6); it was most positively associated with CCL7, CCL18, CXCL10, CCL20, and CCL8.

### 3.8. Association between drug sensitivity and CCNB2

This study identified a significant correlation between *CCNB2* expression and drug sensitivity (Supplementary Table 6). Specifically, *CCNB2* overexpression was associated with increased IC50 values for AZD2014 (Fig. 8A), AZD2014 (Fig. 8B), AZD8055 (Fig. 8C), ipatasertib (Fig. 8D), MK-2206 (Fig. 8E), ribociclib (Fig. 8F), and selumetinib (Fig. 8G). In addition, *CCNB2* overexpression was related to decreased IC50 values for AZD7762 (Fig. 8H), MK-8776 (Fig. 8I), cisplatin (Fig. 8J), camptothecin (Fig. 8K), topotecan (Fig. 8L), ibrutinib (Fig. 8M), savolitinib (Fig. 8N), and talazoparib (Fig. 8O). Therefore, accurate predictions could enhance the treatment effect for patients with BRCA.

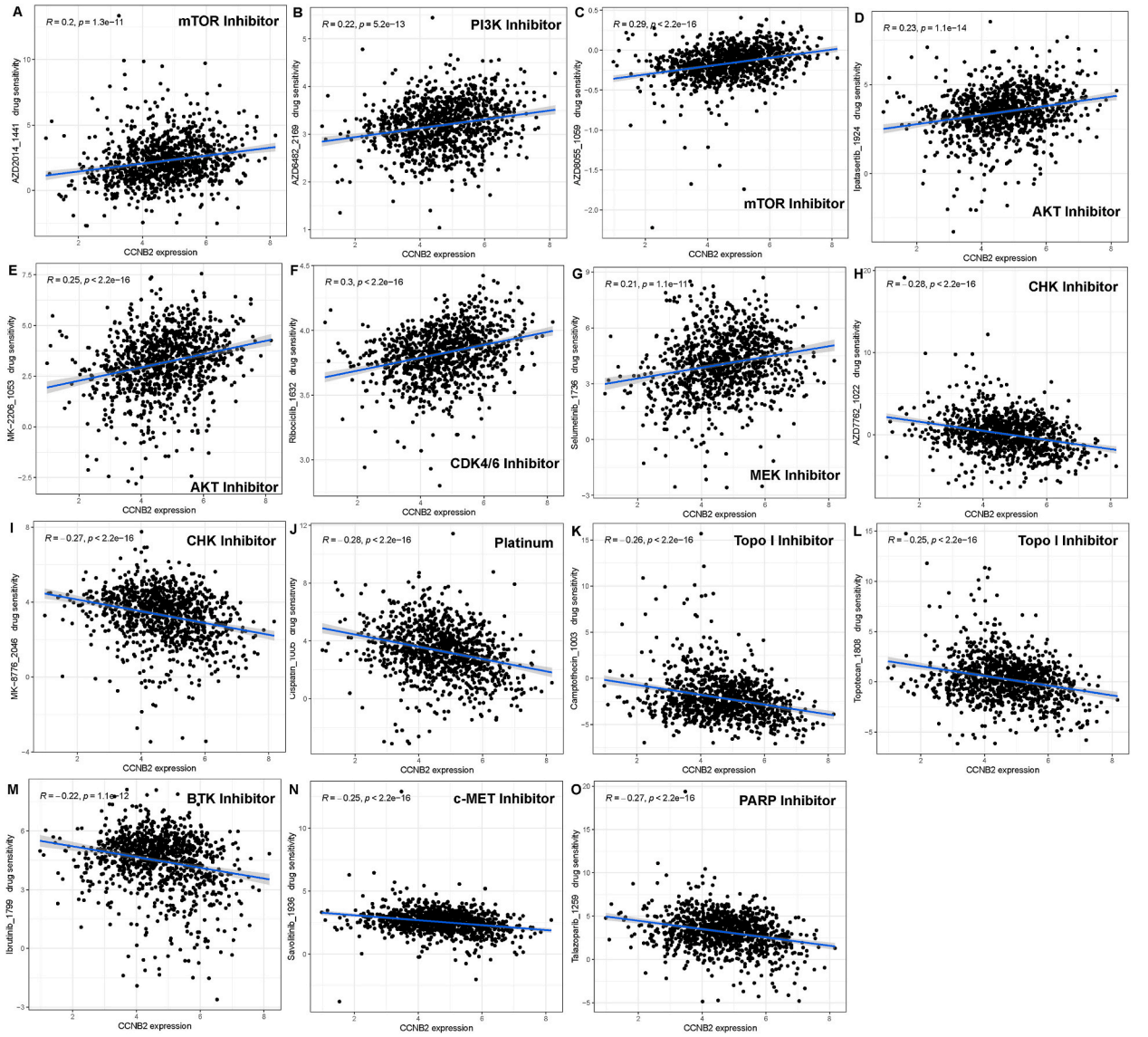


**Fig. 8. The correlation between the drug sensitivity of common clinical anti-tumor drugs and the expression level of CCNB2.** CCNB2 was positively correlated AZD2014 **(A)**, AZD6482 **(B)**, AZD8055 **(C)**, Ipatasertib **(D)**, MK-2206 **(E)**, Ribociclib **(F)**, Selumetinib **(G)**, whereas negatively correlated with AZD7762 **(H)**, MK-8776 **(I)**, Cisplatin **(J)**, Camptothecin **(K)**, Topotecan **(L)**, Ibrutinib **(M)**, Savolitinib **(N)**, Talazoparib **(O)**.

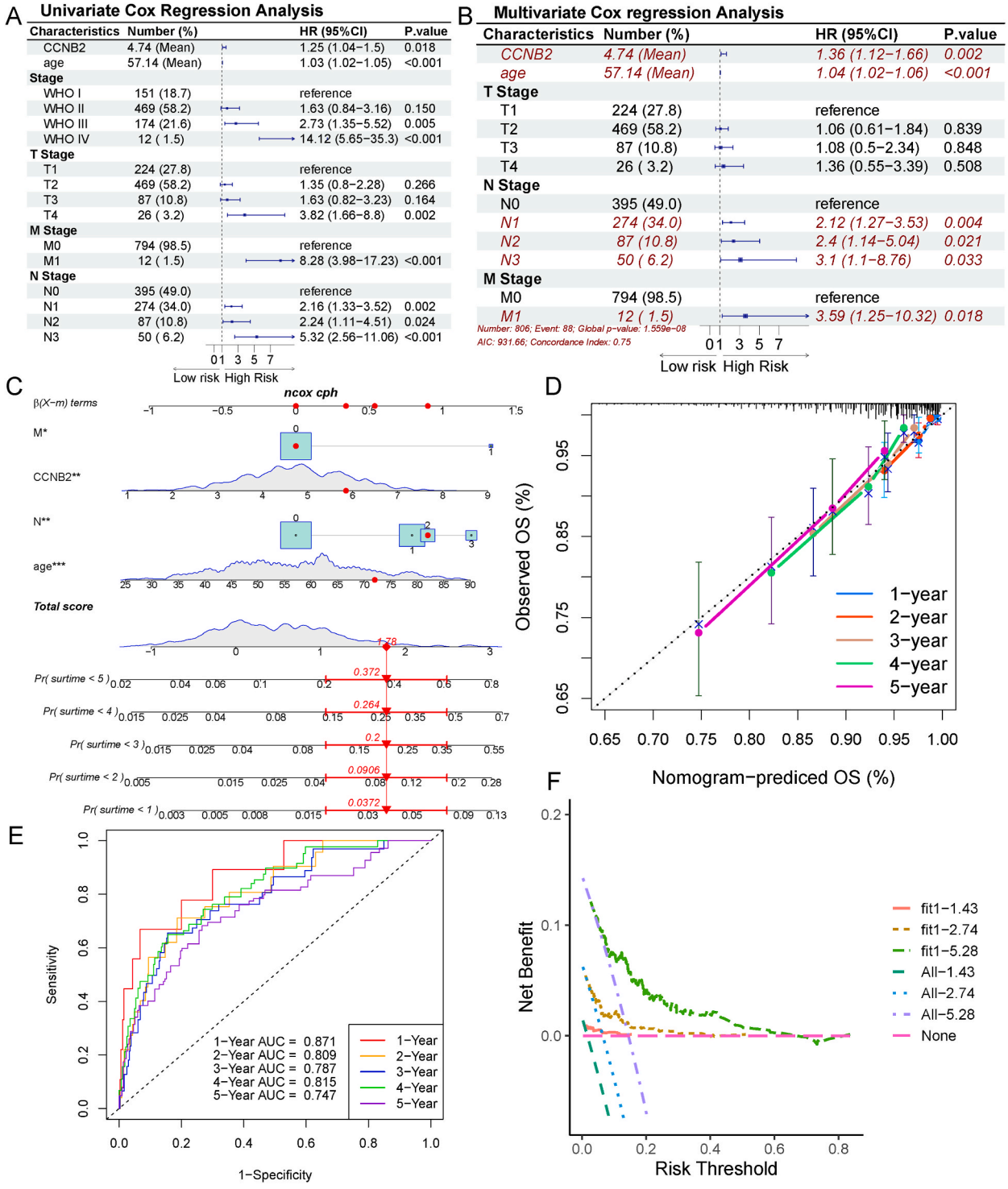


**Fig. 9. Prognostic analyses and nomogram construction.** **(A–B)** Univariate **(A)** and multivariate **(B)** Cox regression analyses showing the hazard ratios (HRs) of different factors using forest plots. **(C)** Nomograms predicting the probability value of the 1-, 2-, 3-, 4-, and 5-year survival risk of CCNB2 expression in BRCA. **(D)** Receiver operating characteristic curves of CCNB2 expression level combined with age, N stage and M stage. **(E)** Calibration curve of the nomogram. **(F)** Decision curves for 1-, 3- and 5-year overall survival. **P < 0.01, ***P < 0.001.

### 3.9. Prognostic value of CCNB2 in BRCA

The univariate Cox regression analysis demonstrated a significant association between *CCNB2* expression and overall survival (hazard ratio: 1.25, 95 % confidence interval = 1.04–1.5; p = 0.018; Fig. 9A and Supplementary Table 7). Moreover, *CCNB2* was an independent risk factor for overall survival in the multivariate Cox regression analysis (hazard ratio: 1.36, 95 % confidence interval = 1.12–1.66; p = 0.002; Fig. 9B).

Next, the survival data was integrated with clinical variables (age, N stage and M stage) and the *CCNB2* expression level to construct a prognostic nomogram for predicting an individual's risk after 1, 2, 3, 4, and 5 years (Fig. 9C). The ROC curve showed that the AUC values were 0.871, 0.809, 0.787, 0.815, and 0.747, respectively (Fig. 9E). The calibration curve demonstrated excellent concordance between the actual and predicted survival outcomes (Fig. 9D). For instance, a 72-year-old (66.8 points) female patient with N2 stage (35.1 points) and M0 stage (0 point) BRCA, and an *CCNB2* expression level of 6.806 (60.7 points), has a total score of 162.6 points. Therefore, this patient's estimated 1-, 2-, 3-, 4-, and 5-year survival rates were 96 %, 91 %, 80 %, 74 % and 63 %, respectively (Fig. 9D). Decision curves showed good predictive accuracy for this signature (Fig. 9F).

## 4. Discussion

BRCA is a devastating malignancy and the leading cause of cancer-related deaths among women in most countries. For decades, clinical treatment for BRCA has relied on surgery, with additional support from chemotherapy, radiotherapy, and endocrine therapy. However, discovering molecular markers and new drug targets has created new possibilities for targeted treatments. Currently, gene-targeting therapies for BRCA primarily focus on oncogenes, tumor suppressor genes, and tumor angiogenesis genes. Immunotherapy is also becoming increasingly valuable. Therefore, understanding the roles of immune molecules in the development and progression of BRCA is crucial.

The DEG, survival, and PPI network analyses identified CCNB2 as a key gene in BRCA. Furthermore, comprehensive analysis of overall survival or relapse-free survival data for BRCA from an independent database determined that patients with high CCNB2 expression had a poor overall prognosis compared to those with low expression, aligning with previous studies [24–26]. Univariate and multivariate Cox regression analyses also identified the CCNB2 expression level as an independent prognostic factor for BRCA. Previous studies have found a positive correlation between high expression of CCNB2 and clinical staging [47]. In this research, the prognostic nomogram, ROC curves and decision curves were constructed involving the CCNB2 expression level, age, N stage and M stage, which can help clinicians accurately identify high-risk patients. Furthermore, prominent differences in protein levels were confirmed in BRCA cell lines and tissue samples, which could serve as prognostic markers for BRCA. Cell proliferation assay and invasion assay demonstrated that high CCNB2 expression could enhance the proliferate and invasive ability of breast cancer cells.

Moreover, this study conducted functional enrichment analyses to investigate the function of CCNB2 and its co-expressed genes. Consistent with a previous study, CCNB2 was found to be vital in the cell cycle pathway [48]. Additionally, the co-expressed genes were enriched in the PI3K-Akt-mTOR pathway. PI3K-Akt-mTOR pathway activation is common in BRCA and acts as an oncogenic driver, promoting cell transformation, tumor initiation, development, metastasis, and apoptotic resistance [49]. The drug sensitivity analysis also confirmed the functional enrichment analysis results. PI3K inhibitors (AZD6482), AKT inhibitors (ipatasertib, MK-2206), and mTOR inhibitors (AZD2014, AZD8055) were positively associated with CCNB2 expression. Moreover, increased ROS production promoted $CD4^+$ T cell apoptosis and tumorigenesis, and oxidative distress influenced their immunosuppressive capacity in Tregs. MDSCs are also an excellent example of how ROS mediate immunosuppression in the TME [50]. These results further suggest the potential mining value of the role of CCNB2 in tumor development and the immune microenvironment.

A significant correlation between CCNB2 expression and various immune infiltrating cells, including tumor-associated macrophages, Th2 cells, Tregs, and exhausted T cells, has been reported in hepatocellular carcinoma [51]. Therefore, this study investigated these relationships in BRCA, identifying a positive association between CCNB2 expression and the levels of Th2 cells, Tregs, and MDSCs in BRCA tissues. Previous studies have shown that immune polarization of Th2 cells promotes metastasis in BRCA and is associated with unfavorable genetic properties of the tumor [52]. Tregs, known for their immunosuppressive activity in tumors, pose a major obstacle to effective anti-tumor immunity. In particular, Th2-like Tregs exhibit a high migratory capacity toward chemokines enriched in tumors, potentially contributing to the maintenance of a tumorigenic environment [53]. MDSCs are crucial for creating an immunosuppressive microenvironment, promoting tumor progression, and inducing resistance to anti-tumoral therapies through various non-immunological mechanisms [54]. Conversely, CCNB2 expression was negatively associated with the levels of pDCs, eosinophils, NK cells, neutrophils, and central memory cells in BRCA tissues. Neutrophils contribute to the anti-tumor response by initiating immune responses and directly lysing tumor cells [55]. pDCs secrete interferons, restrain tumor cell growth and migration, and activate NK cells and $CD8^+$ T cells [56]. Interestingly, although activated pDCs may induce anti-tumor reactions in vivo, pDCs in the TME suggest a tumor-promoting effect [57]. Patients with low eosinophil counts have been shown to have an increased risk of recurrent disease and poor specific survival of BRCA compared with those of patients with normal or high eosinophil counts [58]. Most importantly, NK cells, which are essential in the immune response against tumors and their eradication, become dysfunctional in an immunosuppressed TME due to exposure to inhibitory molecules released by cancer cells, resulting in tumor escape [59]. Overall, the analysis of TIICs suggests that CCNB2 may help to create a TME that promotes tumor development, progression, and metastasis by increasing immunosuppressive cells and inhibiting the immune-killing effect.

Previous studies have demonstrated that tumors with mismatch repair deficiencies are more responsive to PD-1 blockade than tumors with proficient mismatch repair [60]. Additionally, the TMB, an essential biological indicator for predicting the immunotherapy response, increases in certain cases of BRCA and is enriched in metastatic tumors [61]. A close correlation was identified

between high CCNB2 expression and increased MSI and TMB levels, suggesting a potential relationship between CCNB2 expression and immune status. Immune cells contribute to tumor growth by promoting immune escape via the upregulation of immune checkpoints and proinflammatory cytokines. T cell exhaustion, characterized by immune suppression within the TME, directly affects T cell function [62]. Notably, this research found a prominent positive correlation between CCNB2 and T cell exhaustion markers, including PD-1, CTLA4, and TIM3; PD-1 and CTLA-4 are vital proteins involved in tumor immune escape [63,64]. These findings indicate that CCNB2 plays a pivotal role in inducing T cell exhaustion and that the upregulation of these markers enhances the suppression of anti-tumor immunity. Furthermore, this study revealed a strong association between CCNB2 expression and most immune checkpoint markers, indicating that CCNB2 may be essential for recruiting and regulating TIICs in BRCA. However, analysis of the chemokine family suggests contradictory conclusions. On the one hand, increased CCL18 and CCL20 expression promotes tumor proliferation and metastasis. In contrast, CXCR3, a known tumor-promoting factor, was significantly negatively correlated with CCNB2 expression. Given the diversity and complexity of the chemokine family, several mechanisms remain unclear. Thus, further exploration of the underlying mechanisms mediating the link between CCNB2 expression and chemokine family members is required.

In addition to the PI3K-Akt-mTOR inhibitors mentioned above, tumors with high CCNB2 expression showed sensitivity to CDK4/6 inhibitors, which are endocrine drugs used in breast cancer treatment. Unfortunately, high CCNB2 expression confers resistance to drugs that cause DNA damage, inhibit DNA repair, and induce tumor apoptosis, possibly because CCNB2 overexpression regulates cell cycle arrest and inhibits the apoptosis of tumor cells. Therefore, targeting CCNB2 in combination with cell cycle inhibitors or immunotherapy could be a promising treatment strategy.

This study corroborates prior research on CCNB2 as a regulator of the cell cycle and confirms its promoting role in tumorigenesis and progression when overexpressed. Furthermore, the study identified the potential involvement of CCNB2 in the cancer tumor microenvironment, whether associated with TMB, MSI, or immune-infiltrating cells, indicating its potential as a biomarker and therapeutic target. Given the limited efficacy of current hormonal therapy and chemotherapy in certain breast cancers, especially triple-negative breast cancer, targeted therapy, particularly immunotherapies targeting the tumor microenvironment, becomes pivotal. Simultaneously, the prognostic model developed in this study and the analysis of drug sensitivity may provide clinicians with treatment references, whether for prognostic inference or combination therapy with other drugs, demonstrating the translational value of CCNB2 as a biomarker. Both in vitro experiments confirming the impact of CCNB2 on tumor initiation and progression, and bioinformatics analyses indicating its role in the tumor microenvironment and immunotherapeutic targeting, demonstrate the broad applicability of CCNB2 as a therapeutic target in both hormone receptor-positive and triple-negative breast cancers. Thus, translating the relationship between CCNB2 and the tumor microenvironment into clinical therapy holds significant promise. This represents a direction for the future efforts, exploring the mechanisms underlying the relationship between CCNB2 and tumorigenesis, as well as the efficacy of its inhibitors and their combination therapy with other drugs.

This study had several limitations. First, retrieving multiple pieces of information from diverse databases introduced systematic bias. Second, the information from TCGA may be biased despite the validation in cell lines and clinical specimens. Third, since the results are based on a public database and computational algorithm, further studies are needed to investigate the function and mechanism of biomarkers in BRCA using in vivo and in vitro approaches. Further efforts should be made to explore the role of CCNB2 in cancer and its value as a potential immune target for anticancer therapy.

## 5. Conclusions

In summary, this study represents the first description of the relationship between CCNB2 and tumor microenvironment as well as immune infiltration in BRCA. Analyses identified novel and clinically significant correlations between CCNB2 and prognosis, immune cell infiltration, immunity markers (e.g., chemokines, immune checkpoint molecules), TMB, MSI, and drug sensitivity. This suggests that the biomarker CCNB2 may serve as a therapeutic target, offering valuable insights into its role in tumor microenvironment and immunotherapy in BRCA.

## Funding

This work was supported by the Fund of Tongji Hospital of Tongji Medical College of Huazhong University of Science and Technology [2201102971].

## Availability of data and materials

The data that support the findings of this study are available from the corresponding author on reasonable request.

## Ethical approval

The studies involving human participants were reviewed and approved by the Ethics Committee of the Huazhong University of Science and Technology (TJ-IRB20220638).

## Consent to participate

The patients provided their written informed consent to participate in this study.

## Consent for publication

Not applicable.

## CRediT authorship contribution statement

**Zonghong Lu:** Writing – review & editing, Writing – original draft, Visualization, Validation, Supervision, Software, Resources, Project administration, Methodology, Formal analysis, Data curation, Conceptualization. **Zhihong Wang:** Writing – review & editing, Visualization, Validation, Resources, Methodology, Formal analysis, Data curation, Conceptualization. **Guodong Li:** Writing – review & editing, Supervision, Resources, Project administration, Methodology, Investigation, Funding acquisition, Conceptualization.

## Declaration of competing interest

The authors declare the following financial interests/personal relationships which may be considered as potential competing interests:Guodong Li reports financial support was provided by the Fund of Tongji Hospital of Tongji Medical College of Huazhong University of Science and Technology (2201102971). If there are other authors, they declare that they have no known competing financial interests or personal relationships that could have appeared to influence the work reported in this paper.

## Acknowledgments

We hold great gratitude toward Dr. Li for the design of the study.

## Appendix A. Supplementary data

Supplementary data to this article can be found online at https://doi.org/10.1016/j.heliyon.2024.e31586.

## References

[1] H. Sung, J. Ferlay, R.L. Siegel, M. Laversanne, I. Soerjomataram, A. Jemal, F. Bray, Global cancer statistics 2020: GLOBOCAN estimates of incidence and mortality worldwide for 36 cancers in 185 countries, CA A Cancer J. Clin. 71 (2021) 209–249, https://doi.org/10.3322/caac.21660.
[2] M. Cao, H. Li, D. Sun, W. Chen, Cancer burden of major cancers in China: a need for sustainable actions, Cancer Commun. 40 (2020) 205–210, https://doi.org/10.1002/cac2.12025.
[3] S. Lei, R. Zheng, S. Zhang, S. Wang, R. Chen, K. Sun, H. Zeng, J. Zhou, W. Wei, Global patterns of breast cancer incidence and mortality: a population-based cancer registry data analysis from 2000 to 2020, Cancer Commun. 41 (2021) 1183–1194, https://doi.org/10.1002/cac2.12207.
[4] A.G. Waks, E.P. Winer, Breast cancer treatment: a review, JAMA 321 (2019) 288–300, https://doi.org/10.1001/jama.2018.19323.
[5] S.K. Yeo, J.-L. Guan, Breast cancer: multiple subtypes within a tumor? Trends Cancer 3 (2017) 753–760, https://doi.org/10.1016/j.trecan.2017.09.001.
[6] R. Hong, B. Xu, Breast cancer: an up-to-date review and future perspectives, Cancer Commun. 42 (2022) 913–936, https://doi.org/10.1002/cac2.12358.
[7] K. Polyak, Breast cancer: origins and evolution, J. Clin. Invest. 117 (2007) 3155–3163, https://doi.org/10.1172/JCI33295.
[8] N. Harbeck, F. Penault-Llorca, J. Cortes, M. Gnant, N. Houssami, P. Poortmans, K. Ruddy, J. Tsang, F. Cardoso, Breast cancer, Nat. Rev. Dis. Prim. 5 (2019) 66, https://doi.org/10.1038/s41572-019-0111-2.
[9] M.A. Franzoi, E. Romano, M. Piccart, Immunotherapy for early breast cancer: too soon, too superficial, or just right? Ann. Oncol. 32 (2021) 323–336, https://doi.org/10.1016/j.annonc.2020.11.022.
[10] R.A. Leon-Ferre, M.P. Goetz, Advances in systemic therapies for triple negative breast cancer, BMJ 381 (2023) e071674, https://doi.org/10.1136/bmj-2022-071674.
[11] S. Wang, Q. Zhang, C. Yu, Y. Cao, Y. Zuo, L. Yang, Immune cell infiltration-based signature for prognosis and immunogenomic analysis in breast cancer, Briefings Bioinf. 22 (2021) 2020–2031, https://doi.org/10.1093/bib/bbaa026.
[12] A.B. Hanker, D.R. Sudhan, C.L. Arteaga, Overcoming endocrine resistance in breast cancer, Cancer Cell 37 (2020) 496–513, https://doi.org/10.1016/j.ccell.2020.03.009.
[13] Y. Bareche, D. Venet, M. Ignatiadis, P. Aftimos, M. Piccart, F. Rothe, C. Sotiriou, Unravelling triple-negative breast cancer molecular heterogeneity using an integrative multiomic analysis, Ann. Oncol. 29 (2018) 895–902, https://doi.org/10.1093/annonc/mdy024.
[14] S. Loibl, P. Poortmans, M. Morrow, C. Denkert, G. Curigliano, Breast cancer, Lancet 397 (2021) 1750–1769, https://doi.org/10.1016/S0140-6736(20)32381-3.
[15] J. Masuda, Y. Ozaki, F. Hara, S. Kitano, T. Takano, Pembrolizumab plus chemotherapy in triple-negative breast cancer, Lancet 398 (2021) 24, https://doi.org/10.1016/S0140-6736(21)00380-9.
[16] A. Bardia, S.A. Hurvitz, S.M. Tolaney, D. Loirat, K. Punie, M. Oliveira, A. Brufsky, S.D. Sardesai, K. Kalinsky, A.B. Zelnak, R. Weaver, T. Traina, F. Dalenc, P. Aftimos, F. Lynce, S. Diab, J. Cortés, J. O'Shaughnessy, V. Diéras, C. Ferrario, P. Schmid, L.A. Carey, L. Gianni, M.J. Piccart, S. Loibl, D.M. Goldenberg, Q. Hong, M.S. Olivo, L.M. Itri, H.S. Rugo, ASCENT clinical trial investigators, sacituzumab govitecan in metastatic triple-negative breast cancer, N. Engl. J. Med. 384 (2021) 1529–1541, https://doi.org/10.1056/NEJMoa2028485.
[17] T. Tang, X. Huang, G. Zhang, Z. Hong, X. Bai, T. Liang, Advantages of targeting the tumor immune microenvironment over blocking immune checkpoint in cancer immunotherapy, Signal Transduct. Targeted Ther. 6 (2021) 72, https://doi.org/10.1038/s41392-020-00449-4.
[18] F. Ye, S. Dewanjee, Y. Li, N.K. Jha, Z.-S. Chen, A. Kumar, null Vishakha, T. Behl, S.K. Jha, H. Tang, Advancements in clinical aspects of targeted therapy and immunotherapy in breast cancer, Mol. Cancer 22 (2023) 105, https://doi.org/10.1186/s12943-023-01805-y.
[19] A. Rizzo, A.D. Ricci, Biomarkers for breast cancer immunotherapy: PD-L1, TILs, and beyond, Expet Opin. Invest. Drugs 31 (2022) 549–555, https://doi.org/10.1080/13543784.2022.2008354.
[20] P. Savas, R. Salgado, C. Denkert, C. Sotiriou, P.K. Darcy, M.J. Smyth, S. Loi, Clinical relevance of host immunity in breast cancer: from TILs to the clinic, Nat. Rev. Clin. Oncol. 13 (2016) 228–241, https://doi.org/10.1038/nrclinonc.2015.215.
[21] L.A. Emens, Breast cancer immunotherapy: facts and hopes, Clin. Cancer Res. 24 (2018) 511–520, https://doi.org/10.1158/1078-0432.CCR-16-3001.
[22] X. Chen, J. Ma, X. Wang, T. Zi, D. Qian, C. Li, C. Xu, CCNB1 and AURKA are critical genes for prostate cancer progression and castration-resistant prostate cancer resistant to vinblastine, Front. Endocrinol. 13 (2022) 1106175, https://doi.org/10.3389/fendo.2022.1106175.

[23] S. Bai, S.E. Taylor, M.A. Jamalruddin, S. McGonigal, E. Grimley, D. Yang, K.A. Bernstein, R.J. Buckanovich, Targeting therapeutic resistance and multinucleate giant cells in CCNE1-amplified HR-proficient ovarian cancer, Mol. Cancer Therapeut. 21 (2022) 1473–1484, https://doi.org/10.1158/1535-7163.MCT-21-0873.

[24] J. Cao, S. Sun, R. Min, R. Li, X. Fan, Y. Han, Z. Feng, N. Li, Prognostic significance of CCNB2 expression in triple-negative breast cancer, Cancer Manag. Res. 13 (2021) 9477–9487, https://doi.org/10.2147/CMAR.S339105.

[25] R. Moradpoor, H. Zali, A. Gharebaghian, M.E. Akbari, S. Ajdari, M. Salimi, Identification of CCNB2 as A potential non-invasive breast cancer biomarker in peripheral blood mononuclear cells using the systems biology approach, Cell J 23 (2021) 406–413, https://doi.org/10.22074/cellj.2021.7053.

[26] C. Sun, S. Lowe, S. Ma, R. Bentley, Z. Zhou, C. Cheng, Q. Zhou, CCNB2 expression correlates with worse outcomes in breast cancer patients: a pooled analysis, Women Health 62 (2022) 655–663, https://doi.org/10.1080/03630242.2022.2106530.

[27] D. Zhang, C. Wang, Z. Li, Y. Li, D. Dai, K. Han, L. Lv, Y. Lu, L. Hou, J. Wang, CCNG2 overexpression mediated by AKT inhibits tumor cell proliferation in human astrocytoma cells, Front. Neurol. 9 (2018) 255, https://doi.org/10.3389/fneur.2018.00255.

[28] S. Li, C. Zhao, J. Gao, X. Zhuang, S. Liu, X. Xing, Q. Liu, C. Chen, S. Wang, Y. Luo, Cyclin G2 reverses immunosuppressive tumor microenvironment and potentiates PD-1 blockade in glioma, J. Exp. Clin. Cancer Res. 40 (2021) 273, https://doi.org/10.1186/s13046-021-02078-3.

[29] Y. Chen, Y. Huang, X. Gao, Y. Li, J. Lin, L. Chen, L. Chang, G. Chen, Y. Guan, L.K. Pan, X. Xia, Z. Guo, J. Pan, Y. Xu, X. Yi, C. Chen, CCND1 amplification contributes to immunosuppression and is associated with a poor prognosis to immune checkpoint inhibitors in solid tumors, Front. Immunol. 11 (2020) 1620, https://doi.org/10.3389/fimmu.2020.01620.

[30] Y. Wang, Y. Liu, L. Xiang, L. Han, X. Yao, Y. Hu, F. Wu, Cyclin D1b induces changes in the macrophage phenotype resulting in promotion of tumor metastasis, Exp. Biol. Med. 246 (2021) 2559–2569, https://doi.org/10.1177/15353702211038511.

[31] A. Colaprico, T.C. Silva, C. Olsen, L. Garofano, C. Cava, D. Garolini, T.S. Sabedot, T.M. Malta, S.M. Pagnotta, I. Castiglioni, M. Ceccarelli, G. Bontempi, H. Noushmehr, TCGAbiolinks: an R/Bioconductor package for integrative analysis of TCGA data, Nucleic Acids Res. 44 (2016) e71, https://doi.org/10.1093/nar/gkv1507.

[32] A. Mayakonda, D.-C. Lin, Y. Assenov, C. Plass, H.P. Koeffler, Maftools: efficient and comprehensive analysis of somatic variants in cancer, Genome Res. 28 (2018) 1747–1756, https://doi.org/10.1101/gr.239244.118.

[33] M.I. Love, W. Huber, S. Anders, Moderated estimation of fold change and dispersion for RNA-seq data with DESeq2, Genome Biol. 15 (2014) 550, https://doi.org/10.1186/s13059-014-0550-8.

[34] M.E. Ritchie, B. Phipson, D. Wu, Y. Hu, C.W. Law, W. Shi, G.K. Smyth, Limma powers differential expression analyses for RNA-sequencing and microarray studies, Nucleic Acids Res. 43 (2015) e47, https://doi.org/10.1093/nar/gkv007.

[35] H. Chen, P.C. Boutros, VennDiagram: a package for the generation of highly-customizable Venn and Euler diagrams in R, BMC Bioinf. 12 (2011) 35, https://doi.org/10.1186/1471-2105-12-35.

[36] T. Wu, E. Hu, S. Xu, M. Chen, P. Guo, Z. Dai, T. Feng, L. Zhou, W. Tang, L. Zhan, X. Fu, S. Liu, X. Bo, G. Yu, clusterProfiler 4.0: a universal enrichment tool for interpreting omics data, Innovation 2 (2021) 100141, https://doi.org/10.1016/j.xinn.2021.100141.

[37] T. Li, J. Fu, Z. Zeng, D. Cohen, J. Li, Q. Chen, B. Li, X.S. Liu, TIMER2.0 for analysis of tumor-infiltrating immune cells, Nucleic Acids Res. 48 (2020) W509–W514, https://doi.org/10.1093/nar/gkaa407.

[38] Z. Gu, L. Gu, R. Eils, M. Schlesner, B. Brors, Circlize Implements and enhances circular visualization in R, Bioinformatics 30 (2014) 2811–2812, https://doi.org/10.1093/bioinformatics/btu393.

[39] Z. Gu, R. Eils, M. Schlesner, Complex heatmaps reveal patterns and correlations in multidimensional genomic data, Bioinformatics 32 (2016) 2847–2849, https://doi.org/10.1093/bioinformatics/btw313.

[40] P. Shannon, A. Markiel, O. Ozier, N.S. Baliga, J.T. Wang, D. Ramage, N. Amin, B. Schwikowski, T. Ideker, Cytoscape: a software environment for integrated models of biomolecular interaction networks, Genome Res. 13 (2003) 2498–2504, https://doi.org/10.1101/gr.1239303.

[41] D. Szklarczyk, R. Kirsch, M. Koutrouli, K. Nastou, F. Mehryary, R. Hachilif, A.L. Gable, T. Fang, N.T. Doncheva, S. Pyysalo, P. Bork, L.J. Jensen, C. von Mering, The STRING database in 2023: protein-protein association networks and functional enrichment analyses for any sequenced genome of interest, Nucleic Acids Res. 51 (2023) D638–D646, https://doi.org/10.1093/nar/gkac1000.

[42] D. Zeng, Z. Ye, R. Shen, G. Yu, J. Wu, Y. Xiong, R. Zhou, W. Qiu, N. Huang, L. Sun, X. Li, J. Bin, Y. Liao, M. Shi, W. Liao, IOBR: multi-omics immuno-oncology biological research to decode tumor microenvironment and signatures, Front. Immunol. 12 (2021) 687975, https://doi.org/10.3389/fimmu.2021.687975.

[43] M. Ramos, L. Geistlinger, S. Oh, L. Schiffer, R. Azhar, H. Kodali, I. de Bruijn, J. Gao, V.J. Carey, M. Morgan, L. Waldron, Multiomic integration of public oncology databases in bioconductor, JCO Clin. Cancer Inform. 4 (2020) 958–971, https://doi.org/10.1200/CCI.19.00119.

[44] B. Ru, C.N. Wong, Y. Tong, J.Y. Zhong, S.S.W. Zhong, W.C. Wu, K.C. Chu, C.Y. Wong, C.Y. Lau, I. Chen, N.W. Chan, J. Zhang, TISIDB: an integrated repository portal for tumor-immune system interactions, Bioinformatics 35 (2019) 4200–4202, https://doi.org/10.1093/bioinformatics/btz210.

[45] M. D, G. Rf, H. Rs, oncoPredict: an R package for predicting in vivo or cancer patient drug response and biomarkers from cell line screening data, Briefings Bioinf. 22 (2021), https://doi.org/10.1093/bib/bbab260.

[46] W. Yang, J. Soares, P. Greninger, E.J. Edelman, H. Lightfoot, S. Forbes, N. Bindal, D. Beare, J.A. Smith, I.R. Thompson, S. Ramaswamy, P.A. Futreal, D.A. Haber, M.R. Stratton, C. Benes, U. McDermott, M.J. Garnett, Genomics of Drug Sensitivity in Cancer (GDSC): a resource for therapeutic biomarker discovery in cancer cells, Nucleic Acids Res. 41 (2013) D955–D961, https://doi.org/10.1093/nar/gks1111.

[47] X. Qian, X. Song, Y. He, Z. Yang, T. Sun, J. Wang, G. Zhu, W. Xing, C. You, CCNB2 overexpression is a poor prognostic biomarker in Chinese NSCLC patients, Biomed. Pharmacother. 74 (2015) 222–227, https://doi.org/10.1016/j.biopha.2015.08.004.

[48] J. Li, J.-X. Tang, J.-M. Cheng, B. Hu, Y.-Q. Wang, B. Aalia, X.-Y. Li, C. Jin, X.-X. Wang, S.-L. Deng, Y. Zhang, S.-R. Chen, W.-P. Qian, Q.-Y. Sun, X.-X. Huang, Y.-X. Liu, Cyclin B2 can compensate for Cyclin B1 in oocyte meiosis I, J. Cell Biol. 217 (2018) 3901–3911, https://doi.org/10.1083/jcb.201802077.

[49] D. Tewari, P. Patni, A. Bishayee, A.N. Sah, A. Bishayee, Natural products targeting the PI3K-Akt-mTOR signaling pathway in cancer: a novel therapeutic strategy, Semin. Cancer Biol. 80 (2022) 1–17, https://doi.org/10.1016/j.semcancer.2019.12.008.

[50] K.B. Kennel, F.R. Greten, Immune cell - produced ROS and their impact on tumor growth and metastasis, Redox Biol. 42 (2021) 101891, https://doi.org/10.1016/j.redox.2021.101891.

[51] Y. Zou, S. Ruan, L. Jin, Z. Chen, H. Han, Y. Zhang, Z. Jian, Y. Lin, N. Shi, H. Jin, CDK1, CCNB1, and CCNB2 are prognostic biomarkers and correlated with immune infiltration in hepatocellular carcinoma, Med. Sci. Monit. 26 (2020) e925289, https://doi.org/10.12659/MSM.925289.

[52] S. Schreiber, C.M. Hammers, A.J. Kaasch, B. Schraven, A. Dudeck, S. Kahlfuss, Metabolic interdependency of Th2 cell-mediated type 2 immunity and the tumor microenvironment, Front. Immunol. 12 (2021) 632581, https://doi.org/10.3389/fimmu.2021.632581.

[53] C. Li, P. Jiang, S. Wei, X. Xu, J. Wang, Regulatory T cells in tumor microenvironment: new mechanisms, potential therapeutic strategies and future prospects, Mol. Cancer 19 (2020) 116, https://doi.org/10.1186/s12943-020-01234-1.

[54] K. Li, H. Shi, B. Zhang, X. Ou, Q. Ma, Y. Chen, P. Shu, D. Li, Y. Wang, Myeloid-derived suppressor cells as immunosuppressive regulators and therapeutic targets in cancer, Signal Transduct. Targeted Ther. 6 (2021) 362, https://doi.org/10.1038/s41392-021-00670-9.

[55] E.B. Eruslanov, P.S. Bhojnagarwala, J.G. Quatromoni, T.L. Stephen, A. Ranganathan, C. Deshpande, T. Akimova, A. Vachani, L. Litzky, W.W. Hancock, J. R. Conejo-Garcia, M. Feldman, S.M. Albelda, S. Singhal, Tumor-associated neutrophils stimulate T cell responses in early-stage human lung cancer, J. Clin. Invest. 124 (2014) 5466–5480, https://doi.org/10.1172/JCI77053.

[56] S.S. Hernández, M.R. Jakobsen, R.O. Bak, Plasmacytoid dendritic cells as a novel cell-based cancer immunotherapy, Int. J. Mol. Sci. 23 (2022) 11397, https://doi.org/10.3390/ijms231911397.

[57] B. Reizis, Plasmacytoid dendritic cells: development, regulation, and function, Immunity 50 (2019) 37–50, https://doi.org/10.1016/j.immuni.2018.12.027.

[58] S. Grisaru-Tal, M. Itan, A.D. Klion, A. Munitz, A new dawn for eosinophils in the tumour microenvironment, Nat. Rev. Cancer 20 (2020) 594–607, https://doi.org/10.1038/s41568-020-0283-9.

[59] B. Cózar, M. Greppi, S. Carpentier, E. Narni-Mancinelli, L. Chiossone, E. Vivier, Tumor-infiltrating natural killer cells, Cancer Discov. 11 (2021) 34–44, https://doi.org/10.1158/2159-8290.CD-20-0655.

[60] D.T. Le, J.N. Uram, H. Wang, B.R. Bartlett, H. Kemberling, A.D. Eyring, A.D. Skora, B.S. Luber, N.S. Azad, D. Laheru, B. Biedrzycki, R.C. Donehower, A. Zaheer, G.A. Fisher, T.S. Crocenzi, J.J. Lee, S.M. Duffy, R.M. Goldberg, A. de la Chapelle, M. Koshiji, F. Bhaijee, T. Huebner, R.H. Hruban, L.D. Wood, N. Cuka, D. M. Pardoll, N. Papadopoulos, K.W. Kinzler, S. Zhou, T.C. Cornish, J.M. Taube, R.A. Anders, J.R. Eshleman, B. Vogelstein, L.A. Diaz, PD-1 blockade in tumors with mismatch-repair deficiency, N. Engl. J. Med. 372 (2015) 2509–2520, https://doi.org/10.1056/NEJMoa1500596.

[61] R. Barroso-Sousa, E. Jain, O. Cohen, D. Kim, J. Buendia-Buendia, E. Winer, N. Lin, S.M. Tolaney, N. Wagle, Prevalence and mutational determinants of high tumor mutation burden in breast cancer, Ann. Oncol. 31 (2020) 387–394, https://doi.org/10.1016/j.annonc.2019.11.010.

[62] S.P. Kubli, T. Berger, D.V. Araujo, L.L. Siu, T.W. Mak, Beyond immune checkpoint blockade: emerging immunological strategies, Nat. Rev. Drug Discov. 20 (2021) 899–919, https://doi.org/10.1038/s41573-021-00155-y.

[63] M.F. Krummel, J.P. Allison, CTLA-4 engagement inhibits IL-2 accumulation and cell cycle progression upon activation of resting T cells, J. Exp. Med. 183 (1996) 2533–2540, https://doi.org/10.1084/jem.183.6.2533.

[64] A. Goodman, S.P. Patel, R. Kurzrock, PD-1-PD-L1 immune-checkpoint blockade in B-cell lymphomas, Nat. Rev. Clin. Oncol. 14 (2017) 203–220, https://doi.org/10.1038/nrclinonc.2016.168.